



Published in final edited form as:

Macromolecules. 2012 November 27; 45(22): 8939–8952. doi:10.1021/ma301568u.

Macromolecular Imaging Agents Containing Lanthanides: Can Conceptual Promise Lead to Clinical Potential?

Joshua Bryson[†], Jeffrey W. Reineke[‡], and Theresa M. Reineke^{§,*}

[†]Techulon Inc. 2200 Kraft Dr., Blacksburg, VA 24060

[‡]Edward Via College of Osteopathic Medicine, Blacksburg, VA 24060

[§]Department of Chemistry, University of Minnesota, Minneapolis, MN 55455

Abstract

Macromolecular magnetic resonance imaging (MRI) contrast agents are increasingly being used to improve the resolution of this noninvasive diagnostic technique. All clinically-approved T₁ contrast agents are small molecule chelates of gadolinium [Gd(III)] that affect bound water proton relaxivity. Both the small size and monomeric nature of these agents ultimately limits the image resolution enhancement that can be achieved for both contrast enhancement and pharmacokinetic/biodistribution reasons. The multimeric nature of macromolecules, such as polymers, dendrimers, and noncovalent complexes of small molecule agents with proteins, have been shown to significantly increase the image contrast and resolution due to their large size and ability to incorporate multiple Gd(III) chelation sites. Also, macromolecular agents are advantageous as they have the ability to be designed to be nontoxic, hydrophilic, easily purified, aggregation-resistant, and have controllable three-dimensional macromolecular structure housing the multiple lanthanide chelation sites. For these reasons, large molecule diagnostics have the ability to significantly increase the relaxivity of water protons within the targeted tissues and thus the image resolution for many diagnostic applications. The FDA approval of a contrast agent that consists of a reversible, non-covalent coupling of a small Gd(III) chelate with serum albumin for blood pool imaging (marketed under the trade names of Vasovist and Ablivar) proved to be one of the first diagnostic agent to capitalize on these benefits from macromolecular association in humans. However, much research and development is necessary to optimize the safety of these unique agents for in vivo use and potential clinical development. To this end, recent work in the field of polymer, dendrimer, and noncovalent complex-based imaging agents are reviewed herein and the future outlook of this field is discussed.

Keywords

contrast agent; macromolecular imaging agent; gadolinium-chelate; MRI; theranostic

MRI and Macromolecular Contrast Agents

Nuclear magnetic resonance imaging (MRI) is a high-resolution, non-invasive tomographic imaging technique that relies on the fundamentals of magnetic resonance. More than 60 million diagnostic MRI scans are carried out every year because soft tissues can be reliably imaged at sub-millimeter resolution¹. Because MRI does not require ionizing radiation to produce high quality soft tissue images, it is a very important tool for both the scientific and medical communities. Indeed, several Nobel prizes from various disciplines have been

*To whom correspondence should be addressed, treineke@vt.edu.

awarded that address both nuclear magnetic resonance fundamentals and their applications for imaging. Nobel prizes were first awarded to Block and Purcell in 1952, then in 1991 to Ernst, later in 2002 to Wüthrich, and finally to Lauterbur and Mansfield in 2003.²

Magnetic resonance imaging relies on probing nuclear spins in the body—specifically, nuclei spins from water protons. Signal intensity in MRI is a function of the local values of both longitudinal relaxation rates ($R_1 = 1/T_1$) and transverse relaxation rates ($R_2 = 1/T_2$).^{3,4} The scope of this review focuses on agents that enhance T_1 relaxation and how to increase signal intensity by reducing this rate. In lipophilic tissues, T_1 relaxation times are quite short—for this reason, the magnitude of the signal in these tissues is much greater than the signal from hydrophilic tissues and vasculature. Because it is desirable to obtain brightened high-resolution images of tissue with high water content and fine vasculature, it is often necessary to administer an agent, such as a paramagnetic substance, that may shorten the relaxation times in these regions. Paramagnetic compounds act as small moving magnets, which allow close water protons to quickly relax (by emitting radio frequencies, the signal that is monitored) to Boltzmann population equilibrium.

Unlike radiotracer imaging, where image “brightness” is dictated by the concentration of radioactive nuclei, MRI relies on water proton relaxation and is amplified by a contrast agent that is present in small concentrations relative to the protons it is influencing.³ There are a number of parameters that dictate contrast agent effectiveness in enhancing the relaxivity of bulk water, including the following: rotational motion (τ_r), proton distance from the paramagnetic ion (r), time of proton localization in the proximity of the paramagnetic ion (τ_m), electron relaxation time in the paramagnetic ion (τ_e), and the number of water molecules directly bound to the paramagnetic center (q). Highly paramagnetic lanthanide metals such as Mn(II) and Gd(III), which are ideal as contrast agents, are typically toxic. To enable their use, these metals must be tightly chelated in a stable structure. Adding a chelate around the ionic metal, however, complicates the relationship between important parameters that dictate contrast agent efficiency by creating “inner sphere” (directly chelated to metal) and “outer sphere” (close proximity but not chelated) water environments (Figure 1). The parameters described above and their relationships to relaxation enhancement are well modeled for Gd(III) chelates by equations developed by Solomon, Bloembergen, and Morgan.⁵

Several common and clinically-used small molecule Gd-chelating agents are shown in Figure 2. When considering the design of a molecule that will chelate Gd(III), several of the parameters mentioned above are controllable, while others are not. The parameters that are dictated by Gd(III) and, therefore, are not controllable are (1) the electronic relaxation, τ_e , and, to a lesser degree, (2) proton distance from the paramagnetic center, r , (typically the preferred Gd-OH₂ bond length). By contrast, parameters that can be controlled/tailored to some degree are (1) rotational motion (τ_r), which should be as close to the Larmor frequency as possible; (2) the number of water molecules directly bound to the paramagnetic center (q), which should be as high as possible without compromising chelate stability; and (3) the residence lifetime of the water molecule in the inner sphere (τ_m), which should be short and is dependent on the coordination environment around the Gd(III) ion.⁵

Clinically-relevant Larmor frequencies have an approximate range of 40–65 MHz at 1.5T, although, higher tesla (3T) MRI is becoming more common, as it enhances signal-to-noise. Small molecule contrast agents “tumble” quickly in solution and have rotational correlation times on the order of picoseconds, which is quite fast compared to clinically-relevant Larmor frequencies. Clinically-used small molecule contrast agents also suffer from long water residence times, except for some novel chelate exceptions developed by the Raymond group, which are discussed in a recent review.⁶ To this end, macromolecular contrast agents

have many promising factors. The focus of this article is to discuss improvement in contrast agent efficiency via macromolecular architectures, which can reduce the rotational correlation times (τ_r) such that the rotational frequency rate becomes closer to clinically-relevant Larmor frequencies, thus improving resolution of this imaging technique.

Other than relaxivity enhancement, several unique properties and potential applications arise from the inclusion of a contrast agent within a macromolecular system. The first unique property that macromolecular environments impart over small molecules is increased blood-pool retention lifetime. Architectures larger than ~5 nm surpass the renal pores and are excluded from rapid blood pool clearance by the kidneys. Improvement in contrast agent pharmacokinetics enables more high resolution imaging techniques and modalities to be carried out for increased accuracy and earlier detection. Furthermore, it is now well understood that macromolecular and nanostructured materials show increase permeability and retention in solid tumors due to the leaky vasculature associated with fast-growing malignancies.⁷ This phenomenon, known as the Enhanced Permeability and Retention (EPR) effect, is being widely utilized in the design of new cancer therapeutic and imaging agents, often comprised of polymers, dendrimers, supramolecular and self-assembled structures.

Polymeric Systems

The first application of macromolecules for use as contrast agents, conducted by Sieving *et al.* in 1990,⁸ involved covalent coupling of commonly-utilized chelates that tightly bind Gd(III). Chelates such as DTPA and DOTA (Figure 2) are structurally conducive to chemical coupling modifications to poly-L-lysine (PLL, degree of polymerization of about 100, Figure 3). The authors demonstrated that about 60 to 90 chelates were attached to the PLL structure and the free amines facilitated cross linking of the macromolecule to human serum albumin. When measured at 10 MHz, the PLL conjugates showed two- to three-fold improvement over monomeric analogs like Gd-DTPA and Gd-DOTA.

Concurrently, Spanoghe *et al.* functionalized a wide array of PLL molecular weights (3,300 – 105,000 Da) and studied relaxation enhancement as a function of molecular weight.^{9,10} They also found relaxation enhancement upon conjugation; however, no relationship between relaxivity enhancement and molecular weight was observed, indicating that rotation correlation times were similar between the different molecular weights of PLL-chelate materials. A gain in rotational correlation time due to macromolecule structure can, however, be limited by the free internal motions occurring in the bonds between the chelate and the polymer backbone, which was likely a factor in this study. Another intrinsic issue with this system is the inability to create PLL materials that are homogeneously-labeled with the chelate structure. While the amount of Gd-chelate on the polymers can be controlled, labeling of the PLL backbone is not regio-controlled, which yields disperse materials with an undefined architecture, likely limiting the feasibility of this approach from a regulatory compliance stance. Despite these drawbacks, more recent work using poly-L-lysine polymers and their derivatives has resulted in the creation of some very elegant systems, such as biodegradable polymeric agents,¹¹ bimodal imaging agents,¹² polymeric micelle tumor beacons,¹³ and pH-responsive MRI probes.¹⁴ Researchers continue to pursue PLL and other homopolymer-based grafted peptides, such as poly-L-glutamic acids,¹⁰ as MRI contrast agent scaffolds. In an interesting study that circumvents the above drawbacks, Meade and coworkers synthesized a series of proteins with discrete molecular weights and defined lysine residue positions that were grafted with Gd-DO3A post synthesis.¹⁵ They were able to demonstrate that relaxivity could be modulated by varying lysine spacing and total polymer length.

Recent examples explore the synthetic versatility of PLL coupled with traditional peptide targeting. Sherry and coworkers synthesized a low molecular weight peptide, comprising a vascular endothelial growth factor receptor 2 (VEGFR2) targeting peptide coupled with a multimeric (Gd(III) = 8) DOTA-PLL-based dendron. They employed this material in mice and demonstrated its utility to image subcutaneous (MDA-MB-231 breast cancer) tumors after systemic administration.¹⁶

Along with PLL modification with Gd(III) chelates, conjugation to polysaccharides was also part of the early work towards polymeric contrast agents. Armitage *et al.* modified dextran moieties with varying molecular weights (9,400 – 487,000 Da) with DTPA-type ligands at high conjugation efficiency (40 – 50 %), as shown in Figure 4.¹⁷ Gd-DTPA-conjugated dextran polymer r_1 values showed modest gains of 4.8 to 7.4 $\text{mmol}^{-1} \text{sec}^{-1}$ (an improvement factor of 1.5 – 2.3) compared to monomeric Gd-DTPA at 100 MHz; however, PLLs with increasing molecular weight yielded decreasing relaxivity values. Although the authors offered no explanation for this effect, it could be due to close Gd(III)-Gd(III) distances or slow rotational rates of the macromolecules.

This issue was later studied further by Rebizak *et al.* in 1998.¹⁸ The authors found that, at lower fields (10 – 20 MHz), relaxivity in these systems would increase as the substitution degree increased—but only to a point, which likely indicates Gd-Gd distances were playing a limiting role.¹⁹ This also confirmed that the rotation rate of this polymer-DTPA complex was slower than 100 MHz. Dextran-DTPA and Dextran-DOTA conjugates were evaluated in rabbits by Siauve *et al.* and found to be non-toxic and to possess advantageous properties as blood pool imaging agents.²⁰ Other *in vivo* work indicates similar observations for other types of Gd-chelate-modified polysaccharides.²¹ Relaxivity gains shown by dextran conjugation warrant further research, but, unfortunately, these conjugates suffer from similar dispersity drawbacks to the PLL conjugates.

Another logical choice for Gd(III)-chelate conjugation and building polymeric imaging agents is polyethylene glycol (PEG) due to its hydrophilicity, biocompatibility, and anti-aggregation properties. Researchers have accomplished this using PEG in the backbone of DTPA-PEG copolymers^{22,23} (Figure 5) or by creating PEG branches off of the parent polymer chain.²⁴ Using these materials, Ladd *et al.* found that relaxivity could be increased as a function of PEG molecular weight.²³ However, these systems show lower relaxivity than PLL and dextran systems of similar molecular weights. This outcome may be attributed to the more flexible backbone associated with PEG. This work also draws correlations between monomer selection, viscosity by polymer shape, and chelate stability, as well as the relationships of these properties to relaxivity. This DTPA-PEG polymer series showed excellent biocompatibility and increased blood pool/tumor retention times when the molecular weight exceeded 20,000 Da. Ye and coworkers²⁵ demonstrated that PEG-DTPA copolymers make suitable hepatic targeting agents because they are renally excluded due to their large size. Because the chelate structures in these polymer structures are directly copolymerized into the backbone, these materials are easier to characterize than the post-modified systems discussed above (PLL and dextran).

Copolymers of DTPA-bis-amide have been developed (Figure 6). The first polymers of this class, developed by Wei and coworkers, consisted of DTPA-bis-amides spaced by methylene unit repeats of various lengths ($n = 4, 5, 10, 12$) containing aliphatic alkyl chains.²⁶ The hydrophobic comonomer in this series of polymers led to some interesting conclusions. First, as the length of the hydrophobic block increased, the relaxivity increased. In addition, for polymers containing a large numbers of comonomers, very high relaxivities were observed, which the authors attributed to amphiphilic self-assembly between the hydrophilic and hydrophobic portions of these polymers. Duarte *et al.* extended this work by

using more rigid linkages and found that increasing the rigidity in the hydrophobic comonomer improved overall relaxivity likely due to the decrease in internal flexible bond movements in the polymer backbone.^{27–28} Other interesting work carried out by Lucas *et al.* involved copolymerization of DTPA with amine-functionalized monosaccharides, creating *poly*-glycoamido-DTPA linear polymers.²⁹ Marginal enhancement was observed at the fields where relaxivity was measured.

To further develop DTPA-containing step-growth polymers, the Lu group has developed blood pool imaging polymers that can be degraded and cleared via reductive-severance of their disulfide bonds.²⁸ These polymers were administered *in vivo* in rat models to determine biodistribution, which were compared with those of several clinically-used small molecule agents. Interestingly, these macromolecular imaging agents yielded similar organ retention profiles to the small molecule agents due to the biodegradability of these polymers; however, some increased retention was observed in the liver.³⁰ It was found in that study that the liver accumulation over a shorter time period was higher for the polymer agent as compared to the small molecular agents. However, the liver accumulation over a longer time period polymeric agent was comparable to current clinically approved agents.³¹ As expected, the macromolecular agents designed to be biodegradable demonstrated a much lower long-term body accumulation than the non-degradable polymeric agents.³²

Work has also been devoted to developing macromolecular T₁ contrast agent systems based on chain-growth-type polymerizations. One of the more elegant examples of this was demonstrated in a paper published by Kiessling and coworkers³³ in which they coupled hydroxypyridonate (HOPO)-based Gd(III) chelates to bicyclic alkenes and polymerized them via ring-opening metathesis polymerization (ROMP), as shown in Figure 7. They chose ROMP due to the high functional group tolerance and control associated with this type of polymerization. They were able to obtain a 40% increase in relaxivity enhancement at 60 MHz compared to the free chelate; however, the degree of polymerization was severely limited (DP = 8 – 30) by steric issues between the ROMP catalyst and the large chelate monomer.

Several groups have developed MRI contrast agent polymers based on free radical polymerization strategies. The first example of this technology was demonstrated in a hydroxypropylmethacrylate functionalized with Gd-DOTA functionalized specifically to quantitate biodistribution and pharmacokinetics of the injected macromolecule and monitor their accumulation in arthritic joints.³⁴ In a similar manner, Semmler and coworkers functionalized DTPA-type chelates with a methacrylamide-type monomers and copolymerized with N-(2-hydroxy propyl)methacrylamide and N-methacryloyl tyrosinamide using AIBN (Azobis(iso- butyronitrile)) as an initiator.³⁵ Interestingly, the relaxivities were independent on polymer molecular weight. *In vitro*, these polymers were non-toxic; however, long-term tissue retention was observed (7.6% of agent over 14 days) in rats, which is considered long and could increase Gd-exposure related risks. However, these structures yielded very high resolution images of fine tumor vasculature. The Sherry group has also carried out some very interesting work with contrast agents created via radical polymerization of acrylamide-based DOTA-chelate monomers.³⁶ The polymers they developed are designed to allow contrast via a Paramagnetic Chemical Exchange Saturation Transfer (ParaCEST)-type mechanism. This is accomplished by polymerizing methacrylate-DOTA-type chelates and probing their ability to suppress bulk water signal. These agents show potential as the first polymer systems to exploit the ParaCEST platform.

Polymeric and multimeric contrast agents have recently been used for a variety of intracellular applications to visualize specific cellular processes and activities. Polymeric Gd(III)-chelating materials have been used to deliver transgenes into mammalian cells via

PLL conjugation to Gd-chelates.³⁷ In this approach the PLL-Gd(III) conjugates were electrostatically coupled with plasmid DNA (pDNA), resulting in formation of a nanoparticle capable of entering the cell and releasing the DNA payload. More recently, theranostic polymers have been developed by Bryson et. al. for nucleic acid delivery into mammalian cells (Figure 8).³⁸ These step-growth polymers compact pDNA into colloidal complexes (polyplexes) and were internalized into cultured cells with high efficiency, however, luciferase transgene expression was lower than anticipated and was attributed to possible barriers in nuclear delivery. This was able to be visualized *in vitro* with these polymers that were chelated with europium III (via polyplex luminescence signal) where most of the signal was localized to the cytoplasm. The polymers created in this study that were chelated with gadolinium III also transfected cells and showed a significantly higher image contrast than nontransfected cells, thus demonstrating potential for both therapeutic delivery and diagnostic imaging and could even be used for *ex vivo* transformations. This may provide a future method for *in vivo* MRI tracking of genetically engineered cells, which is currently a fundamental barrier to the development of new cell-based therapies.

As demonstrated in the work described above, the use of polymers was essential for attaining desired macromolecular benefits and developing contrast agent systems. Despite the fact that these materials can suffer from inherent issues, such as polydispersity and high internal motion, future work should be carried out to address these potential problems using more controlled polymerizations and better polymer design. Nonetheless, the research described herein still represents highly successful approaches to developing macromolecular contrast agents. As such, this area of research warrants continued development, especially in the areas of targeted imaging and drug delivery.

In an innovative study specifically aimed at bypassing the blood brain barrier (BBB), Koffie et al. synthesized poly(n-butyl cyanoacrylate) (PCBA) nanoparticles (NP's) coated with polysorbate 80 for the purpose of delivering various agent types (contrast agents, fluorophores, and antibodies) through the BBB.³⁹ Koffie et al. utilized wild-type and Alzheimer's disease (AD) transgenic mouse models to demonstrate the ability of the NP's to deliver these agents to enhance brain contrast, as well as target-specific lesion-localizing agents. The agents delivered included the DNA-binding dye bis-benzimide (Hoechst 33258), Texas Red, Tryptan Blue, as well as Alexa-488-conjugated 6E10 antibodies, and Gadovist (a Gd-based MRI contrast agent).³⁹ The first three of these were used to enhance amyloid plaques in AD transgenic mice as well as prove the possibility for delivering potential medicinal antibodies to a selected target lesion, while the Gadovist agent was attempted in wild-type mice to demonstrate the ability to deliver MRI contrast agents in sufficient concentration to enhance and enable investigation of the brain. The group also demonstrated that the NP's alone did not induce irreversible or non-specific damage to the BBB. These results open the doorway for the possibility of delivering not only imaging enhancement agents, but also medicinal therapeutics to the CNS.

Dendrimers

Perhaps as extensive in breadth as polymer contrast agent systems, the use of dendrimers has had a significant impact on the field of macromolecular contrast agents. Dendrimers can suffer from the same drawbacks as polymeric systems (e.g., polydispersity and, to a lesser extent, internal flexibility), but they also provide a scaffold with a large molecular volume that can be functionalized with a high number and density of chelates per molecule. One of the first reported dendrimer-contrast agent systems was based on polyamidoamine (PAMAM) dendrimers conjugated to Gd-chelates.⁴⁰ This initial study directly compared PAMAM generation-2 (G2) and -6 (G6) dendrimers that had been functionalized with isothiolcyanobenzyl-DTPA chelating units (Figure 9). The G6 dendrimer had 170 Gd sites

per molecule and a very high 'per Gd(III)' relaxivity of $34 \text{ mM}^{-1} \text{ s}^{-1}$, which was higher than that of G2 ($r_1 = 21.3 \text{ mM}^{-1} \text{ s}^{-1}$) at 25 MHz. The authors later showed that this difference was directly related to gains in rotational correlation time.⁴¹ The authors also showed that the pharmacokinetics of these two dendrimers were quite different. Specifically, the G2 dendrimer behaved similarly to low molecular weight contrast agents in that it was quickly cleared from the blood pool with little tissue retention. In contrast, the G6 dendrimer had a long blood pool enhancement time of 200 min; this is quite lengthy compared to commercially-available Magnevist™ (Gd-DTPA), which exhibits a time of 24 min. Later reports showed that the clearance route of these dendrimers had a generational dependence.^{42,43} Interestingly, G2–G4 showed complete renal clearance, G5 and G6 showed renal and hepatic clearance, and G7–G10 showed only hepatic (with no renal) clearance. Since prolonged retention is ideal for vascular imaging, clearance becomes the determining factor, which will prevent clinical use. Unfortunately, the only candidates that may be plausible for clinical use, based on clearance times and related mechanisms, are the G2-based systems. For this reason, recent attempts to utilize PAMAM-based contrast agents have focused on targeting application with ligand conjugation.^{44,45} The authors also examined hyperbranched diaminobutane (DAB) dendrimers and found that G2 and G3 were the only acceptable systems. Later *in vivo* studies reported interesting specific applications for PAMAM dendrimer-based contrast agents. Brechbiel and coworkers, for example, successfully showed that G8 and higher PAMAM dendrimers can be used as reliable markers for tumor permeability and as tools to demonstrate the effect of external radiation on tumors.⁴⁶ Star and coworkers showed that these dendrimeric contrast agents could be used as early markers to diagnose acute renal failure.⁴⁷ Konda *et al.* showed that PAMAM could be co-functionalized with DO3A and folate ligands to promote selective uptake and imaging of ovarian tumor xenografts.⁴⁸ Importantly, in an elegant study by Merbach and coworkers, it was shown that PAMAM dendrimers could be functionalized in such a way as to make their relaxivity tunable based on the existing pH environment, thus facilitating the development of *in vivo* pH probes.⁴⁹

Other functionalized dendrimers have also been extensively studied as contrast agents. One of the more notable dendrimers is Gadomer-17⁵⁰ (17 refers to its molecular weight of ~17 kDa, Figure 10), developed by Bayer Schering Pharma and sold for research purposes by *in vivo* Contrast. Gadomer-17[®] consists of DOTA-functionalized PLL arms extending from a 1, 3, 5-benzenetricarboxylate core, as shown in Figure 10 and is promising as a blood pool contrast agent. Although the r_1 of this agent was reported to be $11.9 \text{ mM}^{-1} \text{ s}^{-1}$ at 40 MHz, making it better than many low molecular weight contrast agents, it could likely be improved with more rigidity in the dendrimer. Several interesting *in vivo* studies have been carried out with Gadomer-17[®]. Brasch and coworkers, for example, showed that carcinomas displayed a higher uptake of Gadomer-17 compared with Magnevist™; however, neither contrast agent was successful at delineating malignant tissue from benign tissue.⁵¹ In their follow-up work, Kim *et al.* showed that tumor permeability could be measured with perfusion experiments using this dendrimer.⁵² Gadomer-17[®] was also successfully used to selectively enhance lymph node contrast for detecting lymph node metastasis.⁵³ This dendrimer has also been demonstrated as a suitable agent for visualizing pulmonary embolisms in pigs.⁵⁴ Recent work has shown Gadomer-17 to be useful for imaging blockage in microvasculature.⁵⁵

Newer systems based on PLL dendrimers have been created by Fu *et al.* and are currently undergoing clinical trials.⁵⁶ These macromolecules consist of a PEG chain with DTPA-conjugated PLL dendrimers branching from each terminus (Figure 11). These two components facilitate the ability to vary molecular weight and shape by changing either the PEG linker molecular weight or the dendrimer generation. Of the systems evaluated, the highest relaxivity reported ($r_1 = 10.1 \text{ mM}^{-1} \text{ s}^{-1}$) was from the highest generation system,

which consisted of PEG with $M_n=3400$ Da with G5 L-lysine dendrimers on its termini. Although the authors found that they could control blood circulation lifetimes by varying PEG length, they also reported that increasing PEG length did not improve relaxivity. More extensive *in vivo* work indicated that Gd-DOTA analogues of these dendrimers selectively accumulated in breast cancer tissue and could be used to visualize such cancers.⁵⁷

Luo et. al. worked with similar lysine-based architectures and created a series of generation 2, 3, and 4 lysine-based dendritic agents.⁵⁸ Half of the end groups were functionalized with Gd-based DTPA chelates in a controlled manner. These probes were made in both targeted and non-targeted forms. In the targeted form, the other half of the end groups were functionalized with galactose moieties to impart hepatocyte specificity (via targeting the asialoglycoprotein receptor) and the non-targeted form contained carboxybenzyl (Cbz) groups. The greatest contrast enhancement (at 3T) came from the third generation peptide dendrimer decorated with galactosyl moieties *in vitro* and *in vivo*. Both the targeted and non-targeted forms of their generation 3 dendrimers showed the highest level of relative enhanced signal intensity (SI) of MR images of HepG2 (human hepatocellular carcinoma) cells as compared to their equivalents of generation 2 and 4.⁵⁸ All of the targeted agents (with added galactose moieties) showed greater signal intensity levels at all generations as compared to those with the Cbz groups both *in vitro* and *in vivo*. Also, the targeted agents maintained signal intensity increases versus their Cbz counterparts, potentially explained by faster renal clearance of the non-targeted structures. The G3T (generation 3 targeted dendrimer) not only showed the greatest increase in signal, but did so over all other agents at all time intervals scanned (10, 30, and 60 minutes). Promising research was carried out by Fernandez-Trillo et. al to utilize Cu(I)-catalyzed azide-alkyne cycloaddition, to facilitate efficient and effective functionalization of commercially available PEG-based 1st – 3rd generation dendrimers (PEG-[G1 – G3]) with DO3A-Gd chelates.⁵⁹ Interestingly, the chelates were pre-loaded with Gd prior to “clicking” the chelates onto the PEG dendrimer ends. By chelating the Gd prior to dendrimer functionalization, up to 27 Alk-DO3A-Gd were conjugated to the surface groups in yields ranging between 83–90%. The contrast enhancements found with these macromolecules were similar to those of Gadomer-17 (DO3A-Gd chelated), both *in vitro* and *in vivo* (at 7.05T).⁵⁹ Molecular relaxivity increases were experienced for the higher generation dendrimers up to levels approaching Gadomer-17 for the generation 3 PEG-[G3]-(DO3A-Gd) agent. In contrast, ionic relaxivity only increased for the generation 1 and 2 forms, but subsequently decreased for the generation 3 form. *In vivo* studies were carried out on high-grade glioma (brain tumors) in male swiss nude mice. The change in signal intensity (SI) was then averaged for multiple areas of interest, which included areas of glioma in the brain hemispheres of the mouse models. Solutions of the PEG-[G1]-(DO3A-Gd), PEG-[G2]-(DO3A-Gd), and the controls Dotarem and Gadomer-17 were examined. PEG-[G1]-(DO3A-Gd) and PEG-[G2]-(DO3A-Gd) both showed rapid increases in signal intensity following injection and reached their maximum signal intensity values at 4 minutes post-injection. PEG-[G1]-(DO3A-Gd) ultimately showed a maximum change in signal intensity of 44%, while PEG-[G2]-(DO3A-Gd) showed an even better increase at 50%.

Nwe et. al. created macromolecular imaging agents with cystamine core PAMAM dendrimers (G4SS and G5SS) that were loaded with 30 and 58 DOTAs chelated with Gd(III). In addition, they reduced the dendrimer disulfide core and conjugated these structures to the F(ab')₂ portion of the monoclonal antibody (mAb) panitumumab.⁶⁰ The F(ab')₂ mAb-conjugated half dendrimers were created to capitalize on the affinity of these mAb's (in whole or part) to various forms of cancer (i.e. cancers of the colon, lung, pancreas, prostate, and ovaries). These researchers theorized that fragmented portions of panitumumab would show localization to the targeted tumors, while still allowing rather expedient whole body clearance, resulting in lower background noise and enhanced contrast.

Interestingly, at 3T, relaxivity measurements *in vitro* showed marked (4–7 times) increases for the two Gd-DOTA based dendrimers⁶⁰ and less dramatic increases for the two mAb fragment-based half dendrimers, presumably from their lower number of Gd chelates. Although not explored in this research project, the authors mentioned work by Curtet et al.⁶¹ which proposes that with higher generational mAb-Gd conjugates, the higher numbers of mAb's and Gd's would contribute to increased proton relaxation times. However, further testing is needed to confirm the beneficial effects on relaxation incurred by increased numbers of mAb's on potential imaging agents. *In vivo* measurements on the mAb-based agents were carried out on female nude mice at 3T. Qualitative observations were made on the images produced with the various imaging agents and it was found that the higher molecular weight version of the Gd-based (non-antibody) dendrimer showed the greatest improvement in image intensity within the cranial region, while its lower molecular weight alternative imparted a great improvement in signal intensity in the kidneys due to its more rapid clearance. Both antibody-based agents, as well as the higher molecular weight Gd-based dendrimer, proved less than stellar in elucidating vasculature and structures within the cranium. The authors attributed this to higher molecular weight species being unable to bypass the blood-brain barrier.

All of the dendrimers mentioned thus far have their perimeter decorated with Gd-chelates of either the DTPA or the DOTA type. Another approach towards dendronized contrast agents is to put the Gd-chelate at the barycenter of the molecule, which improves relaxivity by drastically slowing its tumbling time. The drawback of this approach is that it eliminates the multimeric nature associated with other dendrimer-based systems. One such agent explored in the literature is P760-Gd,⁶² which is a dendritic molecule with a Gd-DOTA-based core that has PEG arms diverging out from it (Figure 12). The dendritic atmosphere surrounding the chelate imparts a slower rotational rate of 500 MHz ($t_r = 2$ ns), which is approaching that of MRI fields. This slowing of rotational correlation times under experimental conditions led to $r_1 = 23 \text{ mM}^{-1} \text{ s}^{-1}$ at 40 MHz, which is a very high relaxivity result. Similar gains are achieved by incorporating carbohydrate dendron arms from the barycenter.⁶³

Another example of barycenter-based contrast agents can be seen in the low generation dendrimers created by Pierre *et al.* using Gd-HOPO ligands.⁶⁴ A hydrophilic dendrimer environment is ideal for Gd-HOPO, which has fast water exchange and $q = 2$. The relaxivity of these systems at 40 MHz was reported to be $18 \text{ mM}^{-1} \text{ s}^{-1}$, which was a marginal improvement compared with P760-Gd. Minimal improvement was achieved because, even though Gd-HOPO is dendronized, it still rotates at about 4.2 GHz ($t_r = 238$ ps), which is an order of magnitude faster than P760-Gd. Placing contrast agents at dendrimer barycenters is a newer and less-explored approach for creating novel materials with improved properties. Because this approach has already produced well characterized, high-relaxivity agents, the outlook for these types of dendrimers is very good.

Glycocluster and Metallocluster-Based Systems

Glycoclusters have attracted the attention of several research groups due to their ability to mimic biological surfaces, complex stereochemistry, and unique binding/inclusion properties. Because of these features, there is an interest in coupling glycoclusters with contrast agents. Tanaka *et al.* performed an extensive study of DTPA-oligoamine stereochemistry effects on relaxivity.⁶⁵ Unfortunately, the only MRI quantification study they carried out was to a pixel intensity analysis of spin-echo images for each contrast agent synthesized. This type of analysis gives qualitative data, but offers no basis for quantitative comparison between the agents synthesized. Glycoclusters based on cyclodextrin cores have also attracted the attention of the contrast agent community. Song *et al.* synthesized β -cyclodextrins decorated with DOTA chelates, which they suggested would be useful as

intracellular contrast agents.⁶⁶ Srinivasachari et. al. created β -cyclodextrin-containing delivery vehicles of discrete molecular weight⁶⁶ and the same group employed the high-conversion “click” chemistry developed to create glycoclusters utilizing diethylenetriaminetetraacetic acid (DTTA) chelate groups. This resulted in the synthesis of pure glycoclusters with higher relaxivity than other analogues in their class (Figure 13).⁶⁸

Silsesquioxane core PLL dendrimers also represent an exciting new class of clustered-dendritic contrast materials. Kaneshiro and coworkers synthesized generations 1 through 3 (Gd-DOTA-monoamide)-poly-L-lysine octasilsesquioxane dendrimers as well-defined nanoglobular MRI CAs.⁶⁹ The size of the G1, G2, and G3 nanoglobular contrast agents were between 2.0 – 3.2 nm and showed increases in gained relaxivity as the generation was increased (6.4, 7.2, and 10.0 mM⁻¹ sec⁻¹ for G1, G2, and G3). These clusters were further used for enhanced tumor imaging and vascular imaging with G3 showing the best enhancement. Later, these nanoglobular contrast agents were utilized by Tan and coworkers for CLT1-targeted molecular imaging of the fibrin-fibronectin conjugates in the extracellular matrix of tumors. The authors demonstrate profound efficacy in selectively and effectively imaging human breast carcinoma xenografts in female athymic mice bearing.⁷⁰ Prompted by the great promise of this new class of materials, Henig and coworkers developed similar multimeric silsesquioxane clusters, functionalized with tetraazacyclododecane-based chelates, called “Gadoxanes”.⁷¹ The authors carried out thorough characterization of these Gadoxanes, including determining q value, rotational times, water exchange rates, and practical considerations for clinical feasibility, such as shelf-life.

Like glycoclusters metallocluster-based contrast agents have also been developed and studied as contrast agents. Metalloclusters are multimeric Gd-chelate clusters that are self-assembled, using another paramagnetic ion such as Fe(II) or Mn(II), via highly stable chelates such as bipyridine (bpy) and terpyridine (trpy). The enhancement in contrast due to their rigidity is complemented by the enhancement imparted by the central assembly ion. This route towards easily-assembled clusters was first proposed by Jacques *et al.* for the creation of MRI sensors containing endogenous Fe(II).⁷² Others have designed and tested similar cluster types based on bpy-DTTA type chelates,⁷³ trpy-DOTA, porphyrazine,⁷⁴ and trpy-DTPA.⁷⁵ They found these “metallostars” to have extremely high relaxivity despite their relatively lower molecular weight (Figure 14). In the case of bpy-DTTA, which has a relaxivity that is exceptionally high, the increased relaxivity is attributed to the chelate having q = 2, high rigidity, a paramagnetic Fe(II) center, and slower rotational time due to self-assembly. Pierre *et al.* applied similar thinking when designing their Fe(III)-templated self-assembled contrast agents using multimeric HOPO ligand systems assembled with Fe(III) ions.⁷⁶ These systems, like the metallostars, have exceptional nuclear relaxation dispersion profiles and rapidly assemble in the presence of the required Gd(III) and Fe ions.

Non-covalent coupling to blood pool proteins to impart macromolecular properties

A promising approach for imparting macromolecular contrast enhancement effects on a small –molecule chelate is via non-covalent association to physiological proteins of interest, such as serum albumin, fibrin, and collagen.^{77–81} The first highly successful demonstration of this approach was by Lauffer and coworkers in designing the now-clinically-approved “protein-targeting” agent, MS-325,⁸² now marketed under the trade names Vasovist and Ablavar, which selectively binds to serum albumin and gives stunning blood pool images, as shown in Figure 15. Improved relaxivity was observed due to albumin binding, which slowed tumbling rates from gigahertz to megahertz (i.e., closer to MRI Larmor frequencies).⁸³ The creators of MS-325 have translated the successful aspects of its design to other proteins of interest such as fibrin and collagen 1, both of which are prevalent

markers of cardiovascular diseases. A comprehensive review of all work carried out for MS-325 and analogs can be found in a recent review.⁸⁴

Limitations on Clinical Utilization of Macromolecular Contrast Agents

It is important to note that while macromolecular contrast agents provide much promise in enhancing imaging contrast, to date, a macromolecular contrast agent has not been approved for use in humans by the FDA. Unfortunately there are a significant number of obstacles that exist before commercialization of a potential macromolecular contrast agent will occur. Many technical challenges exist with respect to characterizing the long-term safety of these structures. One general limitation observed in many macromolecular systems is lack of total clearance of large molecule systems after administration.⁸⁵ Many macromolecular formulations counter this issue by developing biodegradable materials to prevent accumulation. However, with Gd-based contrast agents, this is a more complex problem due to innate toxicity associated with Gd.

Furthermore, there is growing recognition of the association between the use of gadolinium-containing contrast agents for magnetic resonance imaging and the serious dermal and systemic disease nephrogenic fibrosing dermopathy/nephrogenic systemic fibrosis (NFD/NSF).⁸⁶ Of chief concern towards Gd contrast agents is their ability to play a triggering role of this disease in late-stage renal-impaired patients. Certainly, it will be necessary to evaluate renal function in these patients, in order to determine risk-versus-benefit in terms of elucidating the extent of the disease to both local and distant sites, as well as lymphatic dissemination for more accurate staging and treatment. The pathogenesis of this disease remains unclear at this time, however NSF/NFD has thus far been observed exclusively in patients with kidney disease or renal dysfunction. NSF/NFD leads to thickened, rough and/or hard skin, which can lead to difficult or severely limited limb movement. In some instances, NSF/NFD is a progressive disease that can also lead to death. Also of note, this disease appears when Gd is administered in diethylenetriamine type chelates (Gd-DTPA and Omniscan) and thus far has not been reported for tetraazacyclododecane-type chelates such as Gd-DOTA (Dotarem).⁸⁷

Conclusions

As discussed above, a significant body of work has contributed to our current understanding of macromolecular contrast agents. A better understanding of biological distribution, relaxivity enhancements, and clearance mechanisms has allowed the scientific community to design exquisite macromolecular contrast agents based on polymers, dendrimers, and small molecule agents that form noncovalent interactions with native biological proteins. Future technological improvements in this area will need to include both novel structural design and focus on the Gd-chelate level, to allow the development of chelates that ensure stable metal chelation to avoid toxic side effects, in particular NFD/NFS, faster water exchange rates possibly with higher water coordination (q) values, and that are easy to conjugate into macromolecular structures. Currently, MRI is moving to higher magnetic field strengths and it will be necessary for contrast agents to follow suit that facilitate high resolution image contrast at high fields. Indeed, the ability to tailor macromolecules as imaging agents will continue to provide technological advancements and will certainly include the exciting developments in multifunctional theranostic agents that combine the ability to deliver both therapeutics and diagnostic agents.⁸⁸

Acknowledgments

We would like to acknowledge funding from the NIH (1R21-EB007244).

References

1. Caravan P. *Chem Soc Rev.* 2006; 35:512–23. [PubMed: 16729145]
2. Nobelprize.org
3. Macomber, RS. *A complete Introduction to Modern NMR Spectroscopy.* Wiley; New York: 1998. p. 1-20.
4. Caravan P, Ellison JJ, McMurry TJ, Lauffer RB. *Chem Rev.* 1999; 99:2293–352. [PubMed: 11749483]
5. Aime S, Botta M, Fasano M, Terreno E. *Chem Soc Rev.* 1998; 27:19–29.
6. Datta A, Raymond KN. *Acc Chem Res.* 2009; 42:938–47. [PubMed: 19505089]
7. Matsumura Y, Maeda H. *Cancer Res.* 1986; 46:6387–92. [PubMed: 2946403]
8. Seiving PF, Watson AD, Rocklage SM. *Bioconjugate Chem.* 1990; 1:65–71.
9. Spanoghe M, Lanens D, Dommissie R, Van der Linden A, Alderweireldt. *Magn Res Imag.* 1992; 10:913–17.
10. Ye F, Ke T, Jeong E-K, Wang X, Yongen S, Johnson M, Lu Z-R. *Mol Pharm.* 2006; 3:507–15. [PubMed: 17009849]
11. Wen X, Jackson EF, Price RE, Kim EE, Wu Q, Wallace S, Charnsangavej C, Gelovani JG, Li C. *Bioconjugate Chem.* 2004; 15:1408–15.
12. Huber MM, Staubli AB, Kustedjo K, Gray MHB, Shih J, Fraser SE, Jacobs RE, Meade TJ. *Bioconjugate Chem.* 1998; 9:242–9.
13. Shiraishi K, Kawano K, Minowa T, Maitani Y, Yokoyama M. *J Control Rel.* 2009; 136:14–20.
14. Aime S, Botta M, Crich SG, Giovenzana G, Palmisano G, Sisti M. *Chem Comm.* 1999; 1999:1577–8.
15. Karfeld-Sulzer L, Waters AE, Davis NE, Meade TJ, Barron AE. *Biomacromolecules.* 2010; 11:1429–36. [PubMed: 20420441]
16. Leon-Rodriguez LM, de Lubag A, Udugamasooriya DG, Proneth B, Brekken RA, Sun X, Kodadek T, Sherry AD. *J Am Chem Soc.* 2010; 132:12829–31. [PubMed: 20795620]
17. Armitage FE, Richardson DE, Li KCP. *Bioconjugate Chem.* 1990; 1:365–74.
18. Rebizak R, Schaefer M, Dellacherie É. *Bioconjugate Chem.* 1997; 8:605–10.
19. Rebizak R, Schaefer M, Dellacherie É. *Eur J Pharm Sci.* 1998:243–8.
20. Siauve N, Clément O, Cuénod A, Benderbous S, Frija G. *Magn Res Imag.* 1996; 14:381–90.
21. Helbich TH, Gossman A, Mareski PA, Radüchel B, Roberts TPL, Shames DM, Mühler M, Turetschek, Brasch RC. *J Magn Res Imaging.* 2000; 11:694–701.
22. Desser TS, Rubin DL, Muller HH, Qing F, Khodor S, Zanazzi G, Young SW, Ladd DL, Wellons JA, Kellar KE, Toner JL, Snow RA. *J Magn Res Imag.* 1994; 4:467–72.
23. Ladd DL, Hollister R, Peng X, Wei D, Wu G, Delecki D, Snow RA, Toner JL, Kellar K, Eck J, Desai VC, Raymond G, Kinter LB, Desser TS, Rubin DL. *Bioconjugate Chem.* 1999; 10:361–70.
24. Mohs AM, Wang X, Goodrich KC, Zong Y, Parker DL, Lu Z-R. *Bioconjugate Chem.* 2004; 15:1424–30.
25. Yan G-P, Zhuo R-X, Xu M-Y, Zhang X, Li L-Y, Liu M-L, Ye C-H. *Polym Int.* 2002; 51:892–8.
26. Kellar KE, Henrichs PM, Hollister R, Koenig SH, Eck J, Wei D. *Mag Res Med.* 1997; 38:712–6.
27. Duarte MG, Gil MH, Peters JA, Colet JM, Elst LV, Muller RN, Geraldes CFGC. *Bioconjugate Chem.* 2001; 12:170–7.
28. Zong Y, Guo J, Ke T, Mohs AM, Parker DL, Lu Z-R. *J Control Rel.* 2006; 112:350–6.
29. Lucas RL, Benjamin M, Reineke TM. *Bioconjugate Chem.* 2008; 19:24–7.
30. Wu X, Zong Y, Ye Z, Lu Z-R. *Pharm Res.* 2010; 27:1390–7. [PubMed: 20393871]
31. Wang X, Feng Y, Ke T, Schabel M, Lu Z-R. *Pharm Res.* 2005; 22:596–602. [PubMed: 15846467]
32. Feng Y, Yuda Z, Ke T, Jeong E-K, Parker DL, Lu Z-R. *Pharm Res.* 2006; 8:1736–42. [PubMed: 16850267]
33. Allen MJ, Raines RT, Kiessling LJ. *J Am Chem Soc.* 2006; 128:6534–5. [PubMed: 16704234]

34. Wang D, Miller SC, Sima M, Parker D, Buswell H, Goodrich KC, Kopecková P, Kopecek J. *Pharm Res.* 2004; 21:1741–1749. [PubMed: 15553217]
35. Kiessling F, Heilmann T, Lammers T, Ulbrich K, Subr V, Peschke P, Waengler B, Mier W, Schrenk H-H, Bock M, Schad L, Semmler W. *Bioconjug Chem.* 2006; 17:42–51. [PubMed: 16417250]
36. Wu Y, Zhou Y, Ouari O, Woods M, Zhao P, Soesbe TC, Keifer GE, Sherry AD. *J Am Chem Soc.* 2008; 130:13854–5. [PubMed: 18817395]
37. Kayyem JF, Kumar RM, Fraser SE, Meade TJ. *Chem Biol.* 1995; 2:615–20. [PubMed: 9383466]
38. Bryson JM, Fichter KM, Chu W-J, Lee J-H, Li J, Madsen LA, Reineke TM. *Proc Nat Acad Sci U S A.* 2009; 106:16913–8.
39. Koffie RM, Farrar CT, Saidi L, William CM, Hyman BT, Spires-Jones TL. *Proc Nat Acad Sci USA.* 2011; 108:46, 18837–18842.
40. Wiener EC, Brechbiel MW, Brothers H, Magin RL, Gansow OA, Tomalia DA, Lauterbur PC. *Mag Reson Med.* 1994; 31:1–8.
41. Wiener EC, Auteri FP, Chen JW, Brechbiel MW, Gansow OA, Scheider DS, Belford RL, Clarkson RB, Lauterbur PC. *J Am Chem Soc.* 1996; 118:7774–82.
42. Kobayashi H, Kawamoto S, Jo S–K, Bryant HL, Brechbiel MW, Star RA. *Bioconjug Chem.* 2003; 14:388–94. [PubMed: 12643749]
43. Kobayashi H, Brechbiel MW. *Mol Imaging.* 2003; 2:1–10. [PubMed: 12926232]
44. Zhu W, Okollie B, Bhujwalla ZM, Artemov D. *Magn Res Med.* 2008; 59:679–85.
45. Longmire M, Choyke PL, Kobayashi H. *Cur Topics Med Chem.* 2008; 8:1180–6.
46. Kobayashi H, Reijnders K, English S, Yordanov AT, Milenic DE, Sowers AL, Citrin D, Krishna MC, Waldmann TA, Mitchell JB, Brechbiel MW. *Clin Can Res.* 2004; 10:7712–20.
47. Dear JW, Kobayashi H, Brechbiel MW, Star RA. *Nephron Clin Pract.* 2006; 103:c45–9. [PubMed: 16543755]
48. Konda SD, Aref M, Wang S, Brechbiel M, Wiener EC. *Magn Res Mat Med Biol.* 2001; 12:104–13.
49. Laus S, Sour A, Ruloff R, Toth E, Merbach AE. *Chem Eur J.* 2005; 11:3064–76. [PubMed: 15776490]
50. Roland O, Turrin C-O, Caminade A-M, Majoral J-P. *New J Chem.* 2009; 33:1809–1824.
51. Daldrup-Link HE, Shames DM, Wendland M, Muhler A, Gossman A, Rosenau W, Brasch RC. *Acad Radiol.* 2000; 7:934–44. [PubMed: 11089696]
52. Kim YH, Choi BI, Cho WH, Lim S, Moon WK, Han JK, Weinmann H–J, Chang K–H. *Invest Rad.* 2003; 38:539–49.
53. Misselwitz B, Schmidt-Willich H, Michaelis M, Oellinger JJ. *Invest Rad.* 2002; 37:146–51.
54. Fink C, Ley S, Puderbach M, Plathow C, Bock M, Kauczor H–U. *Eur Radiol.* 2004; 14:1291–6. [PubMed: 14997336]
55. Krombach GA, Higgins CB, Chujo M, Saeed M. *Radiology.* 2005; 236:510–8. [PubMed: 16040908]
56. Fu Y, Raatschen H–J, Nitecki DE, Wendland MF, Novikov V, Fournier LS, Cyran C, Rogut V, Shames DM, Brasch RC. *Biomacromolecules.* 2007; 8:1519–29. [PubMed: 17402781]
57. Cyran CC, Fu Y, Raatschen H–J, Rogut V, Chaopathomkul B, Shames DM, Wendland MF, Yeh BM, Brasch RC. *J Magn Res Imaging.* 2008; 27:581–9.
58. Luo K, Liu G, She W, Wang Q, Wang G, He B, Ai H, Gong Q, Song B, Gu Z. *Biomaterials.* 2011; 32:7951–7960. [PubMed: 21784511]
59. Fernandez-Trillo F, Pacheco-Torres J, Correa J, Ballesteros P, Lopez-Larrubia P, Cerdan S, Riguera R, Fernandez-Megia E. *Biomacromolecules.* 2011; 12:2902–2907. [PubMed: 21728317]
60. Nwe K, Milenic DE, Ray GL, Kim Y, Brechbiel MW. *Molecular Pharmaceutics.* 2012; 9:374–381. [PubMed: 21882823]
61. Curtet C, Bourgoin C, Bohy J, Saccavini J-C, Thédrez P, Akoka S, Tellier C, Chatal J-F. *Int J Cancer Suppl 2.* 1988; 41:126–132.
62. Elst LV, Port M, Raynal I, Simonot C, Muller RN. *Eur J Inorg Chem.* 2003:2495–501.

63. Fulton DA, Elemento EM, Aime S, Chaabane L, Botta M, Parker D. *Chem Commun.* 2006;1064–6.
64. Pierre VC, Botta M, Raymond KN. *J Am Chem Soc.* 2005; 127:504–5. [PubMed: 15643857]
65. Tanaka H, Ando Y, Wada M, Takahashi T. *Org Biomol Chem.* 2005; 3:3311–28. [PubMed: 16132093]
66. Song Y, Kohlmeir EK, Meade TJ. *J Am Chem Soc.* 2008; 130:6662–3. [PubMed: 18452288]
67. Srinivasachari S, Fichter KM, Reineke TM. *J Am Chem Soc.* 2008; 130:4618–27. [PubMed: 18338883]
68. Bryson JM, Chu W–J, Lee J–H, Reineke TM. *Bioconjug Chem.* 2008; 19:1505–9. [PubMed: 18620446]
69. Kaneshiro TL, Jeong E-K, Morrell G, Parker DL, Lu Z-R. *Biomacromolecules.* 2008; 9:2742–8. [PubMed: 18771313]
70. Tan M, Wu X, Jeong E-K, Chen Q, Lu Z-R. *Biomacromolecules.* 2010; 11:754–61. [PubMed: 20131758]
71. Henig J, Toth E, Engelmann J, Gottschalk S, Mayar HA. *Inorg Chem.* 2010; 49:6124–38. [PubMed: 20527901]
72. Jacques V, Desreux JF. *Topics Curr Chem.* 2002; 221:125–60.
73. Livramento JB, Toth E, Sour A, Borel A, Merbach AE, Ruloff R. *Angew Chem Int Ed.* 2005; 44:1480–4.
74. Song Y, Zong H, Trivedi ER, Vesper BJ, Water EA, Barrett AGM, Radosevich JA, Hoffman BM, Meade TJ. *Bioconjugate Chem.* 2010; 21:2267–2275.
75. Costa J, Ruloff R, Burai L, Helm L, Merbach AE. *J Am Chem Soc.* 2005; 127:5147–57. [PubMed: 15810849]
76. Pierre VC, Botta M, Aime S, Raymond KN. *J Am Chem Soc.* 2006; 128:9272–3. [PubMed: 16848429]
77. Caravan P, Das B, Dumas S, Epstein FH, Helm PA, Jacques V, Koerner S, Kolodziej A, Shen L, Sun WC, Zhang Z. *Angew Chem, Int Ed.* 2007; 46:8171–3.
78. Nair S, Kolodziej AF, Bhole G, Greenfield MT, McMurry TJ, Caravan P. *Angew Chem, Int Ed.* 2008; 47:4918–21.
79. Zhang Z, Greenfield MT, Spiller M, McMurry TJ, Lauffer RB, Caravan P. *Angew Chem, Int Ed.* 2005; 44:6766–9.
80. Kunda A, Peterlik H, Krssak M, Bytzek AK, Pashkunova-Martic I, Arion VB. *J Inorg Biochem.* 2011; 105:250–255. [PubMed: 21194625]
81. Henoumont C, Vander Elst L, Laurent S, Muller RN. *J Phys Chem B.* 2010; 114:3689–97. [PubMed: 20175550]
82. Lauffer RB, Parmelee DJ, Dunham SU, Ouellet HS, Dolan RP, Witte S, McMurry TJ, Walovitch RC. *Radiology.* 1998; 207:529–38. [PubMed: 9577506]
83. Caravan P, Cloutier NJ, Greenfield MT, McDermid SA, Dunham SU, Bulte JW, Amedio JC Jr, Looby RJ, Supkowski RM, Horrocks WD Jr, McMurry TJ, Lauffer RB. *J Am Chem Soc.* 2002; 124:3152–62. [PubMed: 11902904]
84. Caravan P. *Acc Chem Res.* 2009; 42:851–62. [PubMed: 19222207]
85. Grobner T. *Nephrol Dial Transplant.* 2006; 21:1104–1108. [PubMed: 16431890]
86. Jones AJS, Cleland JL. *J Cont Release.* 1996; 41:147–155.
87. Canavese C, Mereu MC, Aime S, Lazzarich E, Fenoglio R, Quaglia M, Stratta P. *J Nephrol.* 2008; 21:324–336. [PubMed: 18587720]
88. Kelkar S, Reineke TM. *Bioconjugate Chem.* 2011; 22:1879–1903.

Biographies



Joshua M. Bryson was born in Cincinnati, Ohio in 1981. He received his B.S. in Chemistry from the University of Cincinnati and subsequently obtained his Ph. D. from Virginia Tech under the mentorship of Prof. Theresa Reineke. After graduate school, Dr. Bryson helped launch Techulon Inc. as Principal Scientist and is in charge of directing polymer-mediated nucleic acid delivery initiatives. He is currently working on enabling polymeric delivery technologies in partnerships with major drug companies and the US Department of Defense.



Jeffrey W. Reineke holds a B.S. degree in Biology with a minor in Chemistry from the California State University, Los Angeles and has held analytical chemist positions at BOC Gasses and BASF. For several years thereafter he was employed in the field of forensic science, which inspired him to pursue a degree in medicine. In 2012, Dr. Reineke, D.O. graduated from the Edward Via College of Osteopathic Medicine in Blacksburg, Virginia and is currently pursuing residency options as a general practitioner in Minnesota.



Theresa M. Reineke is the Lloyd H. Reyerson Professor of Chemistry at the University of Minnesota. She received her B.S. degree in Chemistry from the University of Wisconsin-Eau Claire, an M.S. Degree from Arizona State University, and a Ph.D. from the University of Michigan. As an NIH Postdoctoral Fellow at the California Institute of Technology, she was inspired to enter the field of biomaterials research. The Reineke Research Group is devoted to creative development of synthetic macromolecules for targeted drug, nucleic acid, and diagnostic imaging agent delivery. Dr. Reineke also serves as an Associate Editor of *ACS Macro Letters*.

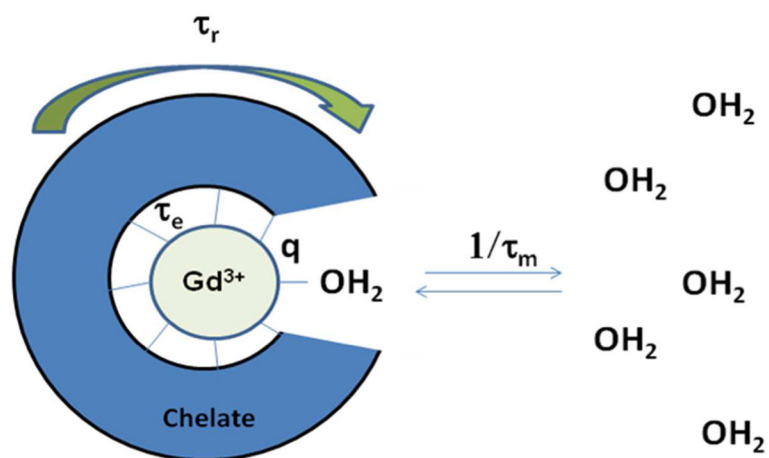


Figure 1. Schematic model showing different contrast agent parameters that apply to relaxivity. The dark blue “cage” surrounding the Gd(III) center represents the chelate. The two parameters commonly altered to improve contrast agents are tumbling motion of the complex, which is represented by τ_r , and water coordination residence lifetime, which is represented with τ_m .¹

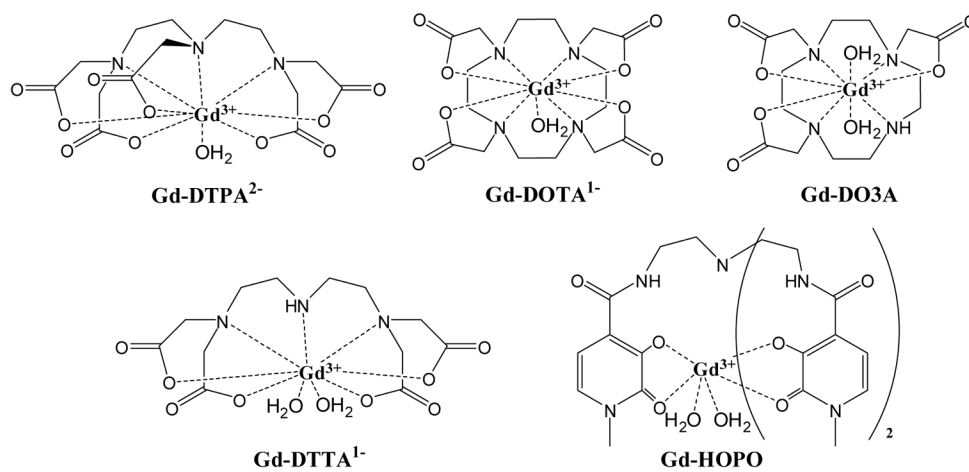


Figure 2. Structures of some common chelating agents for Gd^{3+} that are commonly studied. Gd-DTPA and Gd-DOTA are two of the eight FDA-approved agents currently adapted for clinical use and represent the parent chelate structure utilized in these agents.

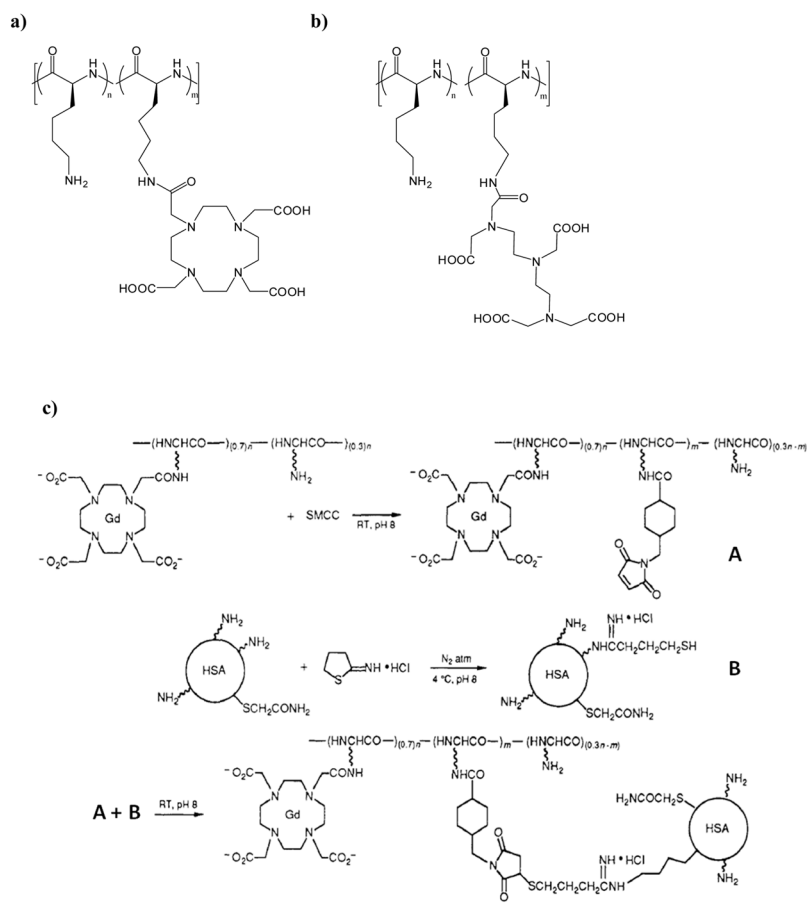


Figure 3. Shown are the structures of a) PLL/PLL-DOTA, and b) PLL/PLL-DTPA random copolymers. C) The coupling reaction used to conjugate the PLL-DOTA macromolecular contrast agent to human serum albumin (HAS).⁸⁻¹⁰ Adapted with permission from Seiving, P. F.; Watson, A. D.; Rocklage, S. M.; *Bioconjugate Chem.* **1990**, *1*, 65-71.⁸

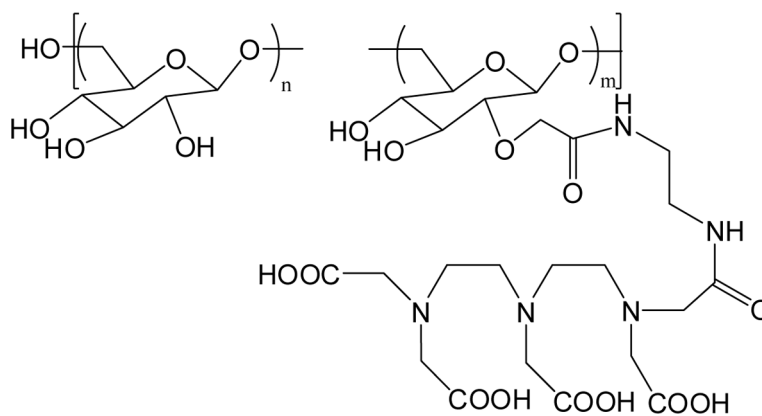


Figure 4.
Dextran polymer randomly functionalized with DTPA.^{17, 18}

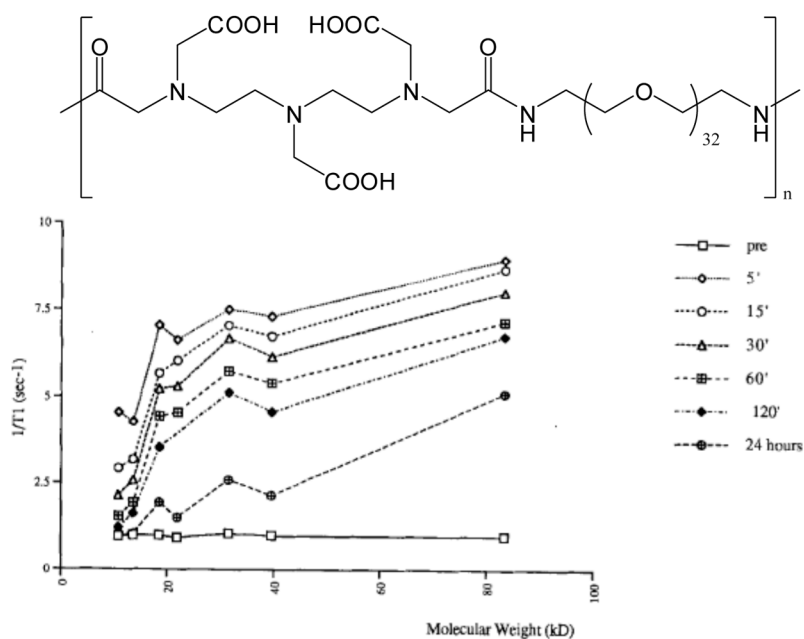


Figure 5.

a) PEG-DTPA copolymers created by Ladd and coworkers, shown without the chelated Gd(III) for clarity. b) Whole-blood R_1 versus molecular weight of the polymer at various time points after injection in rabbits. Reproduced with permission from Desser, T. S.; Rubin, D. L.; Muller, H. H.; Qing, F.; Khodor, S.; Zanazzi, G.; Young, S. W.; Ladd, D. L.; Wellons, J. A.; Kellar, K. E.; Toner, J. L.; Snow, R. A. *J. Magn. Res. Imag.* **1994**, *4*, 467–72.²²

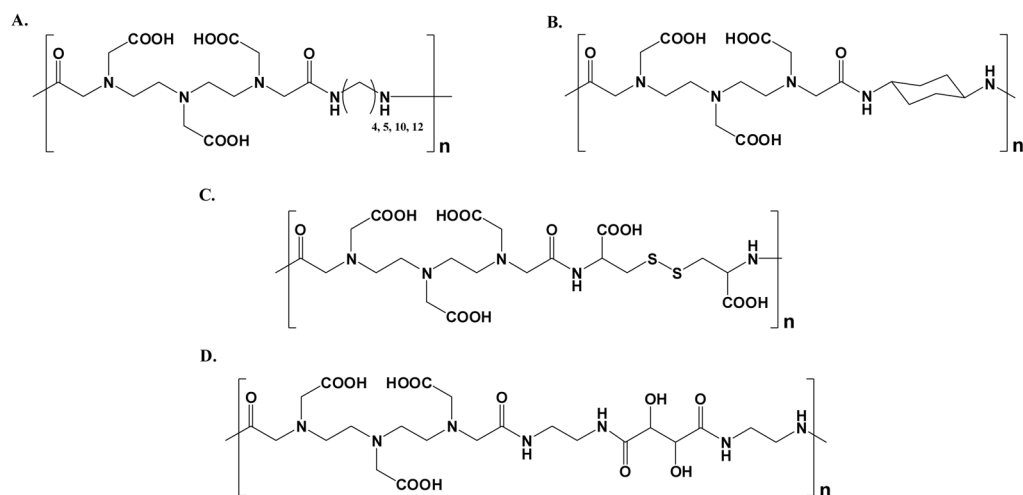


Figure 6. Schematic structures of step-growth DTPA-bis-amide polymers having differing copolymerization chemistry, where the chelates are linked via A) alkyl chains,²⁶ B) a cyclohexyl group,^{27,28} C) disulfide,^{28–32} and D) tartaramide²⁹

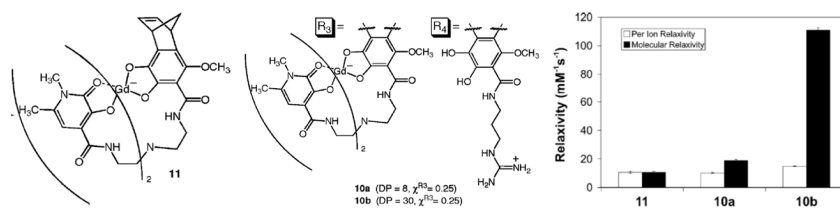
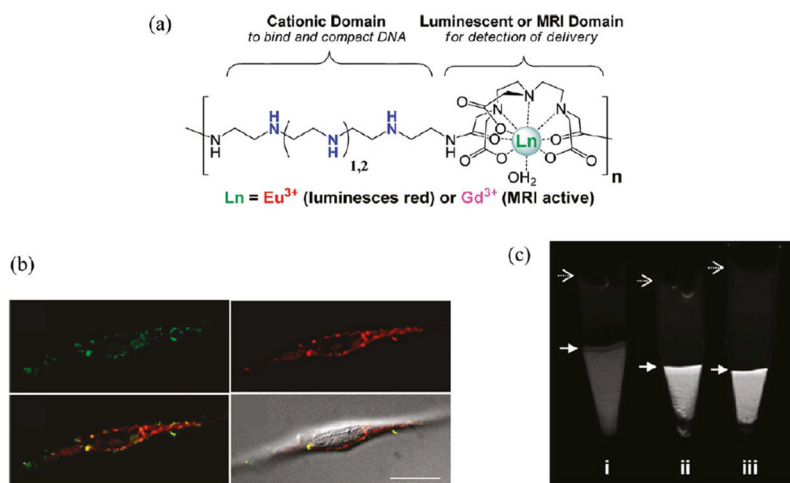
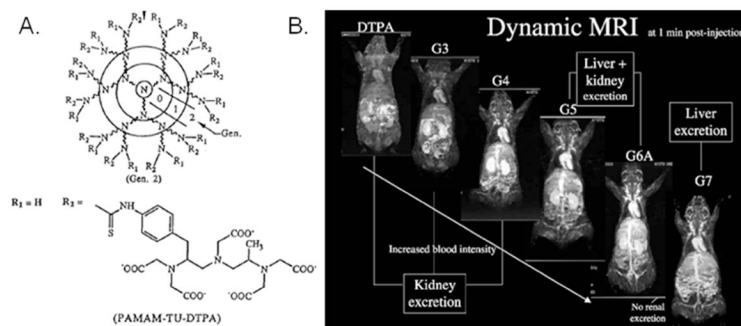


Figure 7. ROMP polymers based on HOPO ligands developed by Allen *et al.*³³ a) Structure of Gd-HOPO ROMP monomer. b) Structure of HOPO random copolymer with DP of 8 and 30 respectively c) Relaxivity of Gd-HOPO monomers and copolymers. Figure adapted from and reproduced with permission from Allen, M. J.; Raines, R. T.; Kiessling, L. J. *J. Am. Chem. Soc.* 2006, 128, 6534–5.³³

**Figure 8.**

(a) Chemical structure of lanthanide- and oligoethyleneamine-containing theranostic polymers for nucleic acid delivery. (b) Deconvoluted confocal microscopy images of HeLa cells transfected with polyplexes containing Eu(III)-chelated polymer (red) and fluorescein isothiocyanate (FITC)-labeled pDNA (green), and their overlay with DIC (differential interference contrast), shows accumulation of polyplexes in the perinuclear region and in cytoplasm. (c) Magnetic resonance (MR) images of cells transfected with two different Gd-containing polymers, (ii) and (iii), compared to untreated HeLa cells (i). Figure adapted and reproduced with permission from Bryson, J. M., Fichter, K. M., Chu, W.-J., Lee, J.-H., Li, J., Madsen, L. A., McLendon, P. M., Reineke, T. M. (2009) *Proc. Natl. Acad. Sci. U.S.A.* 106, 16913–16918.³⁸

**Figure 9.**

A) Diagram describing generations of PAMAM dendrimer and showing chelate connectivity with primary amines.^{41,42} Reproduced with permission from Kobayashi, H.; Kawamoto, S.; Jo, S. -K.; Bryant, H. L.; Brechbiel, M. W.; Star, R. A. *Bioconjug. Chem.* **2003**, *14*, 388–94.

B) *In vivo* rat images showing dendrimer generation effect on contrast agent localization.⁴³ Reproduced with permission from Kobayashi, H.; Brechbiel, M. W. *Mol. Imaging*, **2003**, *2*, 1–10.

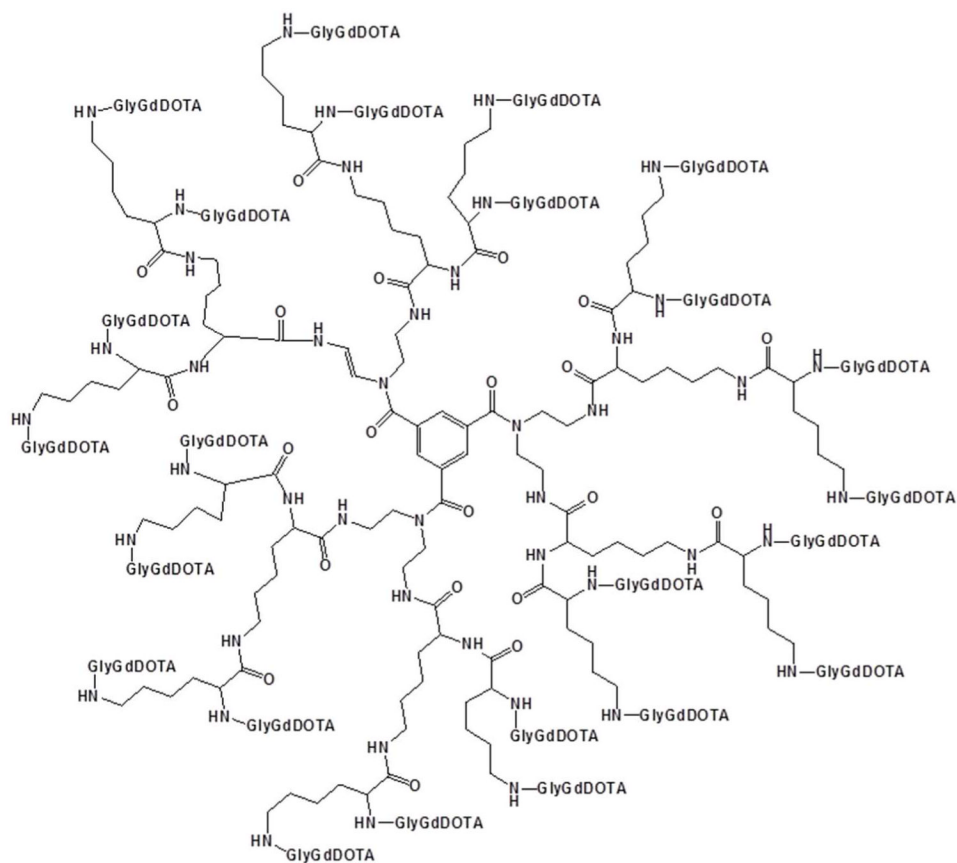


Figure 10.
Chemical structure of Gadomer-17.

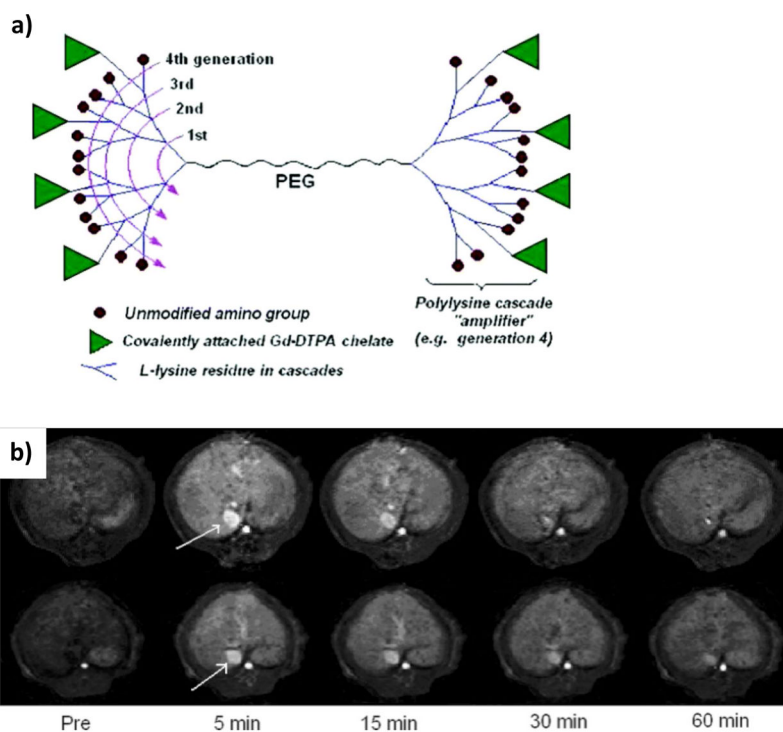
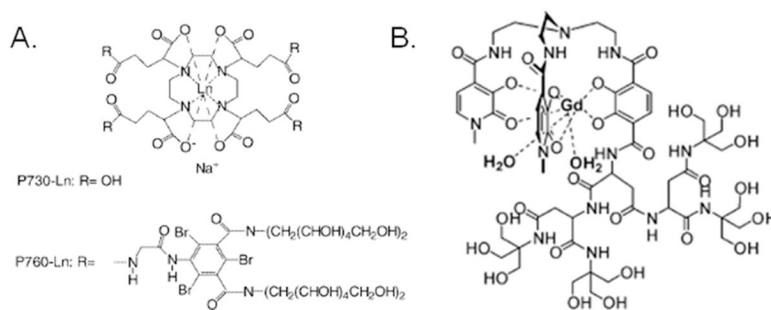


Figure 11.
a) Schematic representation of PLL “bowtie” dendrimers.⁵⁶ Representative enhancement kinetics as revealed by T1-weighted dynamic 3D MR imaging (spoiled gradient recalled sequence, SPGR) of a normal rat at the level of the liver after intravenous injection of PEG12000-Gen4-(Gd-DTPA)8 (upper row) and PEG3400-Gen5-(Gd-DTPA)13 (lower row), respectively, at a dose of 0.04 mmol Gd/kg. The blood enhancement as seen in the inferior vena cava is relatively prolonged being still visible for at least 30 and 60 min, respectively, for these two agents. Their monoexponential blood half-lives were calculated to be 36 and 73 min (mean values), respectively. Figure adapted with permission from: Fu, Y.; Raatschen, H.-J.; Nitecki, D. E.; Wendland, M. F.; Novikov, V.; Fournier, L. S.; Cyran, C.; Rogut, V.; Shames, D. M.; Brasch, R. C. *Biomacromolecules* 2007, 8, 1519–29.⁵⁶

**Figure 12.**

A) P760 dendrimer by Muller *et al.*,⁶² (Adapted with permission from Elst, L. V.; Port, M.; Raynal, I.; Simonot, C.; Muller, R. N. *Eur. J. Inorg. Chem.* **2003**, 2495–501. Copyright 2003 Wiley Publishing)⁶² and B) HOPO dendrimer from Pierre *et al.*⁶⁴ (Adapted from 63. Pierre, V. C.; Botta, M.; Raymond, K. N. *J. Am. Chem. Soc.* 2004, 127, 504–5. Copyright 2004 American Chemical Society)⁶⁴

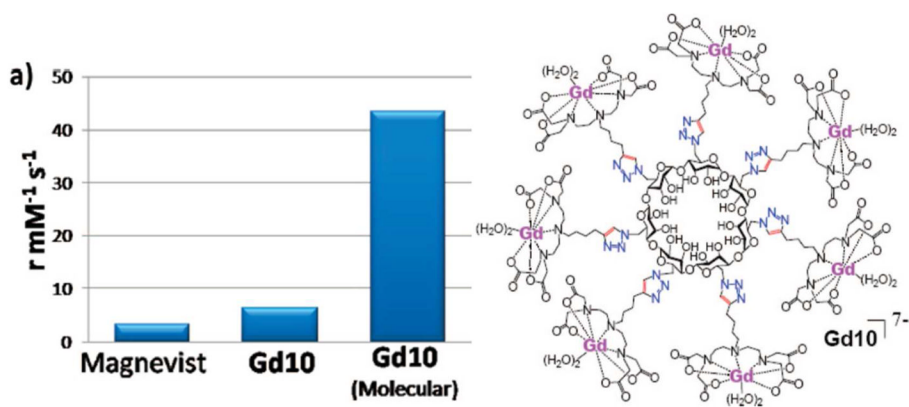


Figure 13.

a) Relaxivity enhancement comparison. b) Structure of the glycocluster chelate **Gd10** developed by Bryson et. al.⁶⁸ Figure adapted from Bryson, J. M.; Chu, W.-J.; Lee, J.-H.; Reineke, T. M. *Bioconjugate Chem.* 2008, 19, 1505–9 with permission. Copyright 2008 American Chemical Society.⁶⁸

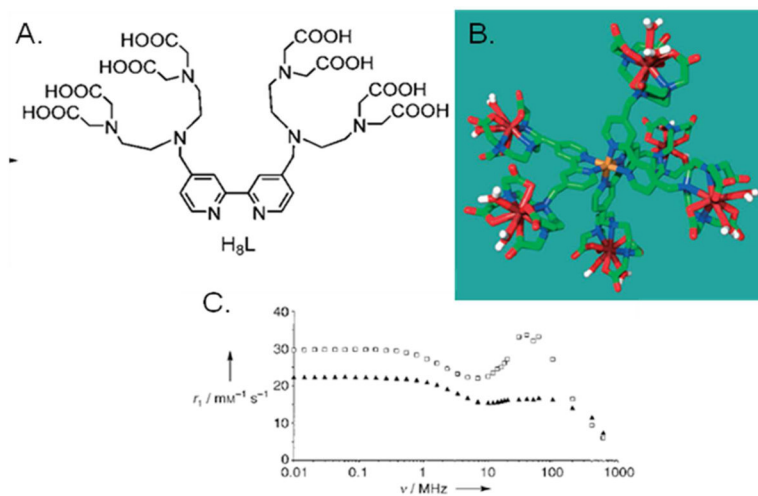


Figure 14. Metallostars developed by Livramento et. al.: A) bpy-DTTA ligand, B) a framework molecular model after ligand assembly with Fe(II) and Gd(III), and C) their NMRD profiles for Gd-DTTA-bpy without Fe(II) (black triangles) and with Fe(II) (white circles).⁷³ Figure adapted from Livramento, J. B.; Toth, E.; Sour, A.; Borel, A.; Merbach, A. E.; Ruloff, R.; *Angew. Chem. Int. Ed.* 2005, 44, 1480 with permission. Copyright 2005 Wiley Publishing.⁷³

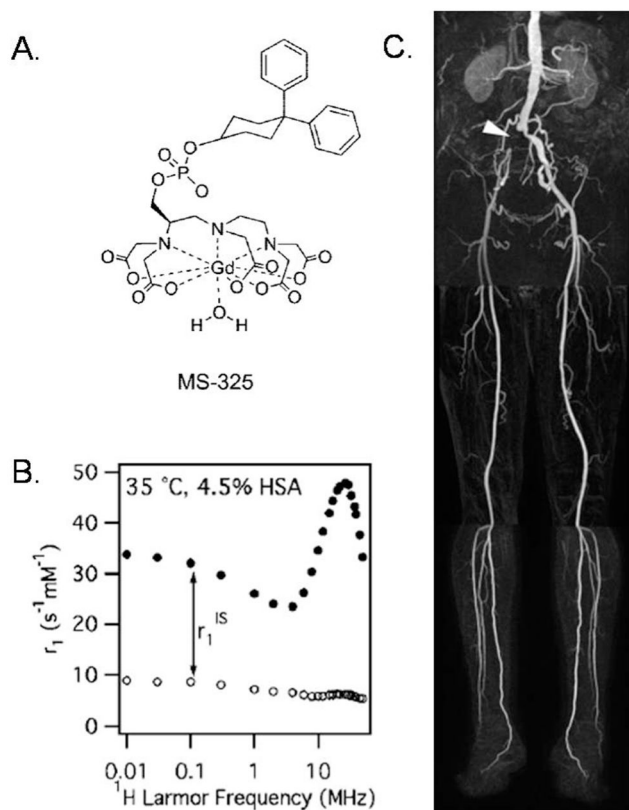


Figure 15.

A) Contrast agent MS-325 that noncovalently binds to serum proteins and forms a macromolecular structure developed by Lauffer and coworkers (marketed as Vasovist and Ablivar). B) NMRD profile of MS-325 (black circles) and MS-325 with water binding site blocked (white circles), both in serum. C) Blood pool image attained with MS-325 in a human subject.⁸⁴ Figure Adapted with permission from Caravan, P.; *Acc. Chem. Res.* 2009, 42, 851–62, copyright 2009 American Chemical Society.⁸⁴